Colloids and Surfaces A: Physicochem. Eng. Aspects 382 (2011) 139–144

Contents lists available at ScienceDirect

Colloids and Surfaces A: Physicochemical and Engineering Aspects

journal homepage: www.elsevier.com/locate/colsurfa

Synthesis of new fluorinated foaming particles

S. Faure [a,*], S. Volland [a], Q. Crouzet [b], G. Boutevin [b], C. Loubat [b]

[a] CEA, Nuclear Energy Division/Center of Marcoule DTCD/SPDE/LPAD, Bagnols/Cèze, France
[b] SPECIFIC POLYMERS, Clapiers (34), France

ARTICLE INFO

Article history:
Received 30 September 2010
Received in revised form
22 December 2010
Accepted 6 January 2011
Available online 18 January 2011

Keywords:
Foam stability
Foaming particles
Fluorinated grafting agent
Radioactive decontamination

ABSTRACT

This paper describes how to synthesise new hydrophobic foaming particles by grafting short fluorinated phosphonic acid (3 carbons) on commercial hydrophilic alumina particles.

The short grafting fluorinated agent CF_3–CFH–CF_2–P(O)$(OH)_2$ preparation is detailed. The corresponding hydrophobic foaming particles are easily prepared by acidic–alkaline grafting using this molecule. "Bikerman foams" are easily generated by air sparging through an aqueous suspension of fluorinated alumina particles. The expansion ratio of the foam could be greater than 20. On a free drainage configuration, relatively dry foams were obtained with a high life time, more than 10 h. The mechanism of stabilisation proposed to describe the role of the particles is based on the attachment of the particles at the air–water interface.

1. Introduction

1.1. Nuclear context—decontamination foam

In the frame of the future dismantling of nuclear facilities, the foam decontamination process has been assessed as an alternative technique to liquid decontamination. These aqueous foams can be viewed as a dispersion of air bubbles in the reactive liquid, stabilised by surface-active species adsorbed at the gas–liquid interfaces. Because decontamination foam is a non-stable two-phases fluid with the aqueous phase representing around 10–15% of the total volume, it strongly decreases the amount of chemicals used during the decontamination processes and the secondary nuclear waste volume [1]. Moreover using foams allows the decontamination of complex shaped facilities.

A decontamination foam comprises at least one surfactant to generate the foam and one or more chemical reactants to achieve the elimination or dissolution of the radioactive deposit on the solid surface [2]. Indeed these deposits can be solubilised by successive liquid rinses with specific aqueous solutions containing alkaline, acidic, or even oxidizing species to dissolve greasy deposits or to corrode the surfaces on micrometric thicknesses.

The foam structure is described by Plateau rules stating that the liquid films between the bubbles meet threefold to form Plateau borders, these latter intersecting four by four at nodes [3]. The liquid thus flows through a continuous network of interconnected channels. Foams age because of several interrelated physical processes, namely drainage of liquid in films and channels, disproportion and coalescence of bubbles. Gravity acts as the main driving force for drainage of wet foams, and capillary suctions between films and Plateau borders gradually increase for lower liquid contents. The progressive thinning of the liquid films eases both the gas diffusion from smaller to larger bubbles driven by their different internal pressures and the further breakage of foam lamellae (coalescence).

From 2000 to 2005, a new decontamination process, called "static foam process", was developed using new foams avoiding the collapse of the foam that can be detrimental to its decontamination efficiency. This was achieved by using biodegradable non-ionic surfactants: alkyl polyglucosides (APGs) and viscosifiers such as xanthan gum [2]. The viscosifier allows increasing the foam lifetime and thus the contact time of chemical reactants with the contaminated walls [4]. Indeed, even though they enclose only about 10% of the reactive liquid in their whole volume, these foams still display similar dissolution rates. Their efficiency is determined by their ability to remain sufficiently wet during the required decontamination time. Other studies showed that slowing down foam ageing can be achieved by increasing liquid viscosity or using poorly soluble gas to reduce gas diffusion [5].

Since 2006, we are trying to develop foams stabilised by mineral particles to reduce or replace both the organic surfactants and organic viscosifiers agents used in usual decontamination foams. One major aim is to generate for nuclear industry more "mineral" aqueous foams easier to treat by simple filtration of the foaming particles.

* Corresponding author.
E-mail address: sylvain.faure@cea.fr (S. Faure).

0927-7757/$ – see front matter © 2011 Elsevier B.V. All rights reserved.
doi:10.1016/j.colsurfa.2011.01.014

1.2. Choice of our particles as foams stabilisers

1.2.1. Foaming particles at the air–water interface

Since 2000, numerous studies aimed to understand stabilisation mechanisms of particle-stabilised foams. The most cited particles stabilizing air–water interface have included silica, clay, alumina, barium sulfate, calcium carbonate, titanium oxide, modified cellulose, carbon and latex [6–9]. Most of the particles are commercial and hydrophilic with non-foaming properties. In order to stabilise air–water interface, the major approach studied to modify their wettability is adsorption of surfactant molecules on particles surfaces in order to increase hydrophobicity [10–12]. The attachment of the particle to the air–water interface depends on the particle radius and the contact angle θ the particle makes with the interface [13]. For instance, for $\theta = 90^\circ$ and particle size of 200 nm, there is a strong particle attachment of 5×10^5 kT. In some case, the difficulty is to attribute the foamability that could be due to both modified surface wetting particles and free surfactants [12].

Without discussing the size and the shape of the particles which influence foamability and stability of the foam, the pre-aggregation in water and adsorption of particles to bubbles during foaming is complex to clarify [10]. Particle aggregation may or may not be advantageous to foam generation and stability. This aggregation was observed by Binks co-workers: the silanisation of commercial fumed silica particles by reaction with dimethyldichlorosilane in the presence of water was studied [13,14]. The foams are generated with an Ultra-Turrax dispersing system immerged inside a water suspension containing 8.6 g/L of sylilated silica particles. Only wet foams with 30% of water were obtained. Aggregation of the particles at the interface and in the bulk decreases the drainage kinetic and stabilises the foams.

Over particles cannot create aggregates in water but are able to slow down or stop the size evolution of the bubbles. Indeed Alargova et al. developed polymer rod-like particles synthesized from epoxy-type photoresist SU-8 (MicroChem, MA) [15]. These anisotropic and hydrophobic polymer microrods ($\theta = 80^\circ$) of diameter less than 1 μm and length of a few tens of micrometers generated dry stable foams during weeks. This superstabilisation effect is due to the rods at the interface that entangle, overlap, and sometimes form small oriented domains: the interface becomes more rigid avoiding contraction of the bubbles and gas diffusion.

Another way more complex to synthesize foaming particles is to prepare Janus Particles [16]. For instance, Reculusa et al. have prepared hybrid dissymmetrical colloidal particles with a controlled morphology combining both organic and inorganic parts. These particles could be used to generate foams [17].

Finally, Stocco et al. recently try to elucidate the remarkable stability of foams generated from dispersions of partially hydrophobic nanoparticles (fumed silica) without any additives [18]. By using ellipsometry and Brewster angle microscopy, the team provides evidence for a pronounced adsorption barrier for the particles and a network-like structure in the interface at sufficiently high concentrations. They observe this structure also in freely suspended films drawn from the same particle dispersions.

1.2.2. Particles studied in our laboratory

The study of decontamination foams stabilised by colloidal particles at CEA is an emergent activity which has been undertaken for almost four years [19]. Particles are believed to increase the foamability of the suspensions and the lifetime of the foams.

Our strategy in order to formulate decontamination foams stabilised by mineral particles followed two ways:

the first way to find new hydrophilic "macro-particles" to slow down the drainage and replace the stabiliser based on organic xanthan gum [20].

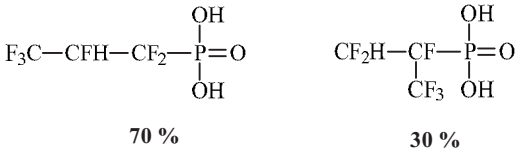

Scheme 1. Isomers of the fluorophosphonic acid used as grafting agent (1,1,2, 3,3,3 Hexafluoropropyl phosphonic acid and [1-(difluoromethyl)-1,2,2,2-tetrafluoroethyl]phosphonic acid).

the more recent way detailed in this paper to obtain new foaming particles easy to prepare.

1.2.3. Hydrophilic "macro-particles"

In 2006, we started to explore how we could modify the drainage behaviour of aqueous foams with totally hydrophilic fumed silica nanoparticles used to formulate gel. While for high particulate concentrations the liquid flow can be slowed down owing to viscosity effects, we show that much less concentrated systems, but possessing peculiar physicochemical properties, can also strongly modify the drainage behaviour [20]. As the foam dries, these highly porous agglomerates called "macro-particles" exhibit typical size and intrinsic yield-stress properties. They are captured by the bubbles during the foam generation stage and thereby form local plugs with growing yield stresses that eventually prevent them from flowing with the liquid out of the foam. They are retained according to a geometrical criterion based on the particle/bubble sizes ratio. The drainage curves of the foams display significant retention rates for the suspension during several hours, an effect that is enhanced for higher particles concentrations.

1.3. Foaming particles at the air–water interface

It has been recently shown that alumina particles can be in situ hydrophobized upon surface adsorption of short-chain carboxylic acids at acidic pH conditions [11,12]. These molecules are electrostatically adsorbed onto the particle surface thanks to their hydrophilic head-group [21], leaving the hydrophobic tail in contact with the aqueous medium. The degree of particle hydrophobization depends on the amount of adsorbed carboxylic acid and the length of the hydrophobic tail [12].

To extend this approach we select a headgroup (phosphonic acid) which is able to engage chemistry reaction on particle surface by formation of covalent links. Schwartz et al. have shown that phosphonic acids can react with a variety of metal oxide surfaces to yield, ultimately, phosphonate monolayer films [22,23].

The in situ hydrophobization of alumina particles was accomplished using fluorophosphonic acid (cf. Scheme 1).

Our aim is to prepare easily foaming particles by simple acid–alkaline grafting of short fluorinated chains (3 carbons) on commercial alumina particles, as depicted in Fig. 1.

By washing these particles with acetone, the free phosphonic acid not grafted on the particles is eliminated. Different grafting rates could be reached by controlling the initial mass of fluorinated acid used.

2. Experimental

2.1. Grafting agent synthesis

2.1.1. Reactants

Hexafluoroproprene (HFP) was supplied by Air liquide (France), dimethyl hydrogen phosphonate and di-tert-butyl peroxide were purchased by Aldrich (Saint Quentin Fallavier, France), and were used as received.

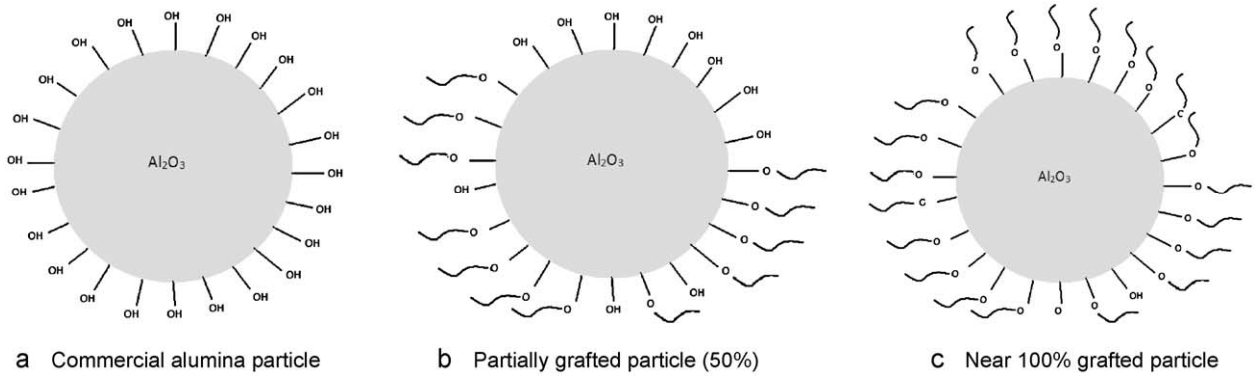

Fig. 1. Grafting of short hairy chains CF_3–CFH–CF_2–P(O)$(OCH_3)_2$ on alumina particles. Particle surface hydrophobicity increases with the number of grafted chains.

2.1.2. Reactions

2.1.2.1. Synthesis of CF_3–CFH–CF_2–P(O)$(OCH_3)_2$. To obtain a suitable amount of HFP monoadduct, the telomerization was carried out in a 300 mL Parr Hastelloy Autoclave (height: 12 cm; internal diameter: 8.5 cm) equipped with a manometer, a rupture disk, inner and outlet valves. The open autoclave was then charged with 1.44 g (0.01 mol) of di-tert-butyl peroxide, 110 g (1 mol) of dimethyl hydrogen phosphonate DMEHP, sealed and purged with nitrogen. After cooling in a liquid nitrogen/acetone mixture, the medium was evacuated and 50.0 g (0.33 mol) of HFP was introduced by double weighing (i.e., the difference of weight after and before feeding the autoclave with TFP). The mixture was heated to 140 °C for 7 h. The maximum pressure reached 12×10^5 Pa. After reaction, the overall HFP conversion was ca.78%, according to the recovered HFP. After cooling down to room temperature, the autoclave was chilled in an ice bath. The unreacted HFP was then vented to a weight dry ice trap and the vessel opened. After evaporation of the byproducts, the total product mixture was fractionally distilled. 50 g (0.24 mol) of CF_3–CFH–CF_2–P(O)$(OCH_3)_2$ was obtained.

2.1.2.2. Synthesis of CF_3–CFH–CF_2–P(O)$(OH)_2$. 21.35 g (0.104 mol) of CF_3–CFH–CF_2–P(O)$(OCH_3)_2$ was introduced in a round bottom flask with 102.22 g (1.036 mol) of HCl 35% and 60 mL of methanol. The mixture was heated to 80 °C during 10 h. After that, subsequent distillation of methanol and water conducted to a slightly yellow oil composed of CF_3–CF_2–CFH–P(O)$(OH)_2$.

2.1.2.3. Apparatus and analysis of products. The structures of the telomers were determined by NMR spectroscopy at room temperature.

The ^{1}H, ^{19}F, and ^{31}P NMR spectra were recorded on a Bruker AC-300 instruments using deuterated chloroform, and tetramethyl silane or $CFCl_3$, as the solvent and internal references, respectively.

2.1.2.4. 1,1,2,3,3,3 Hexafluoropropyl phosphonic acid CF_3–CFH–CF_2–P(O)(OH). b.p. 108–110 °C/20 mmHg; ^{1}H NMR (Acetone D6) δ: CF_3–CFH_c–CF_2-P(O)$(OH)_2$: 5.8 ppm (1H); ^{19}F NMR (Acetone D6) δ: CF_{3a}–CFH–CF_2-P(O)$(OH)_2$: −75 ppm (3F), CF_3–CF_bH–CF_2-P(O)$(OH)_2$: −215 ppm (1F), CF_3–CFH–CF_{2d}-P(O)$(OH)_2$: −126 ppm (2F); ^{31}P NMR (Acetone D6) δ: CF_3–CFH–CF_2-P_e(O)$(OH)_2$: 0.8 ppm (1P)

2.1.2.5. [1-(difluoromethyl)-1,2,2,2-tetrafluoroethyl]phosphonic acid. b.p. 108–110 °C/20 mmHg; ^{1}H NMR (Acetone D6) δ: CF_3–CF(P(O)$(OH)_2$)–CF_2H_i: 6.5 ppm (1H); ^{19}F NMR (Acetone D6) δ: CF_{3f}–CF(P(O)$(OH)_2$)–CF_2H: −72 ppm (3F), CF_3–CF_g(P(O)$(OH)_2$)–CF_2H: −198 ppm (1F); CF_3–CF(P(O)$(OH)_2$)–CF_{2h}H: −131 ppm (2F); ^{31}P NMR (Acetone D6) δ: CF_3–CF(P_e(O)$(OH)_2$)–CF_2H: 1.8 ppm (1P)

2.2. Colloidal particles grafting

The colloidal particles used in this study were acquired from the following supplier: γ-Al_2O_3 - Sasol North America (grade APA 0.5). Giving by the supplier, the average size is 400 nm and specific surface is 8.5 $m^2\,g^{-1}$ (cf. Fig. 2).

A reproducible protocol is followed to prepare the suspensions containing 100 g L^{-1} of particles with a 0.3% weight ratio of grafting agent on alumina. Equal weights (10 g of alumina in 88 g of water) of suspensions are stirred in identical recipes (diameter 5.8 cm, at a fixed speed 9000 rpm (Ultra-Turrax)) during 3×30 s. The pH value is not adjusted (pH 6.8).

The mixture is simply heated at 90 °C and stirred with a Rayneri (60 mm deflocculating rotor blade). A solution of grafting agent (0.03 g in 2 g of water) is added slowly in the mixture and reaction is pursuing during 2 h. The initial concentration of grafting agent is 1.3×10^{-3} mol L^{-1}. White foam appears at the top of the suspension during stirring.

By ICP-AES analysis of phosphorus, the grafting rate obtained is assumed to be inferior to 40%. The following studies are performed on this partially grafted particle (cf. Fig. 1b).

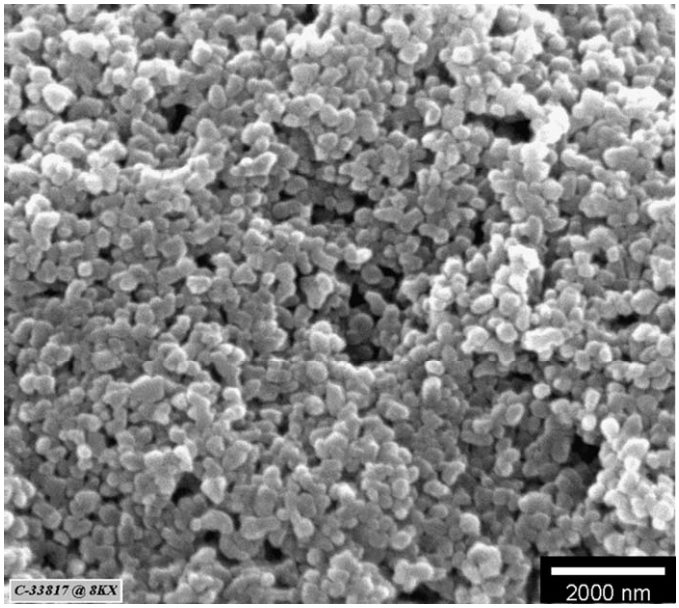

Fig. 2. Picture of primaries particles (Ceralox APA 0.5) by SEM shared by the supplier Sasol North America.

Scheme 2. Telomerization of hexafluoropropene (HFP).

2.2.1. Characterization

The size and zeta potential of particle were determined by using Zetasizer Nanoseries from Malvern Instruments. The surface tension of the suspensions was measured using the pendant drop in air method (TECLIS, France).

Foamability and drainage were studied by conductivity and image analysis with the Foamscan provided by Teclis (need of 25 mL suspension sample volume to generate foam).

3. Results and discussion

3.1. Grafting agent characterization

Phosphorusbearing fluorinated derivatives are known for their applications in the field of complexing agents. Many investigations dealing with the synthesis of perfluorinated phosphonic acid have been described in the literature. Among these methods, the telomerization reaction has proved to be an easy method to prepare such derivatives. Haszeldine et al. studied the peroxide addition of DEHP to different fluoroalkenes, such as TFE, CTFE, VDF, hexafluoropropene (HFP) [24]. In our case, we chose the HFP because of its structure entirely composed of fluorine or carbon. More recently Kostov et al. studied the radical telomerization of TFP [25].

Radical telomerization of hexafluoropropene (HFP) with dimethyl hydrogen phosphonate (DEHP) was initiated by di-tert-butyl peroxide (DTBP) at 140 °C, as follows in Scheme 2:

The first adduct of the telomerization of HFP was synthesized in an autoclave by using di-tert-butyl peroxide (DTBP) as the initiator (mainly 3% in initial molar ratio about HFP: $Co = [DTBP]_o/[HFP]_o = 0.03$). The initial mixture was composed of an excess amount of dimethyl hydrogen phosphonate (DEHP) versus HFP and (defined as $R = [DMEHP]/[HFP]_o = 3.0$). Thus, at 140 °C, the initial pressure in the 300 mL autoclave did not exceed 12 bar.

After evaporation of the HFP and DMEHP, the total product mixture was analyzed by NMR ^1H, ^{31}P and ^{19}F. The ^1H NMR spectrum of the monoadduct shows the presence of both isomers, which exhibit the formulae showed in Schema 1. The formation of both isomers can be deduced by NMR analysis (^1H NMR, ^{19}F NMR) as seen in Fig. 3.

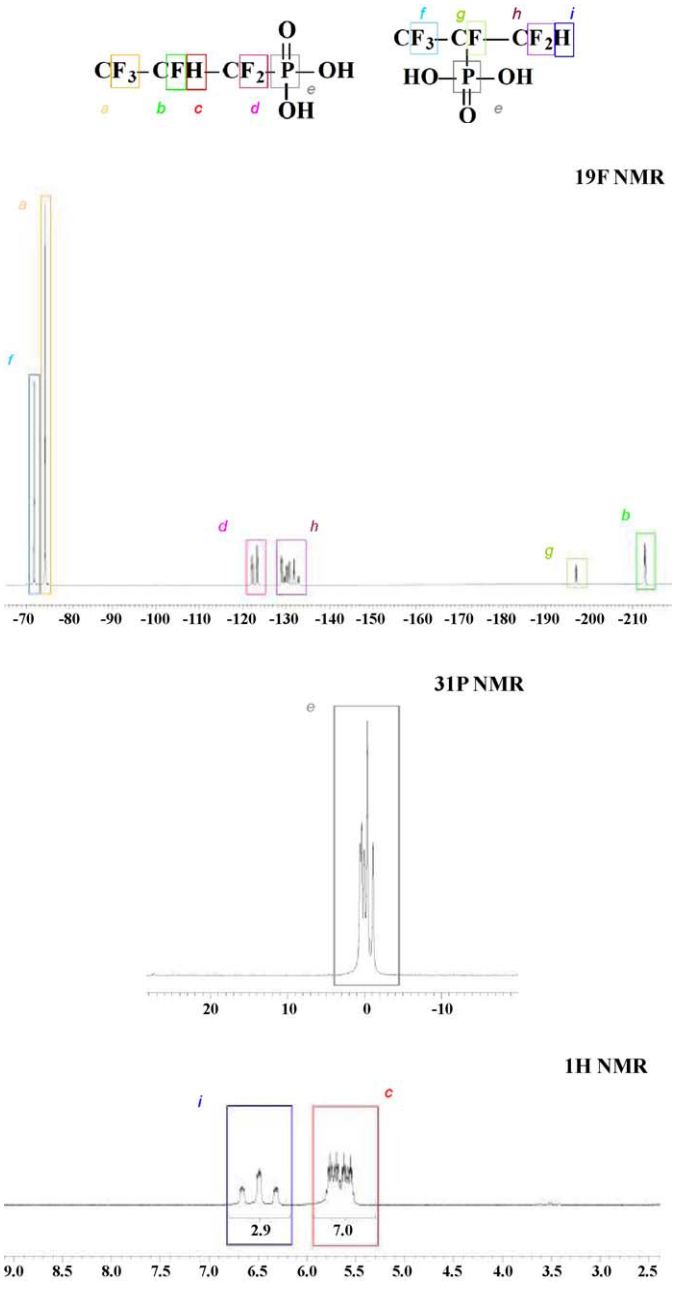

Fig. 3. ^{13}P, ^{19}F and ^1H NMR spectra of grafting agent isomers (cf. II-1 for data).

3.2. Size and surface charge of the particles

The CERALOX alumina particles are suspended in water under agitation. At pH 6.8 in deionised water, the zeta-potential of alumina is close to 35 mV and no aggregation of the primary colloidal particles was observed (cf. Fig. 4). A deflocculating Ultra-Turrax was used in order to carry the best dispersion. The mean size of the particles stays as expected around 400 nm.

For the partially grafted particles, a new 5.6 μm size population is observed and attributed to the aggregation of the grafted particles (cf. Fig. 5). Ultra-Turrax dispersing permits to reduce the amount of 5.6 μm aggregates but re-aggregation is observed in less than 1 h.

This agglomeration could be attributed to the success of the partial grafting reaction: the presence of grafted fluorinated chains induce possible specific attraction which remains unclear. Indeed, the small decreasing of the zeta-potential close to 29 mV cannot explain by itself this agglomeration.

3.3. Suspension surface tension

Even if surface tension measurements with particles at the air–water interface are known to be questionable, Ravera et al. claimed that an apparent surface tension can be measured by drop shape tensiometer [26,27].

The surface tension measured with a pendant drop versus time of suspensions containing 10 g L^{-1} of ungrafted and partially grafted particles are shown in Fig. 6.

Surface tension decreases slowly for the commercial particles (3 mN m^{-1} in 8 h). Complementary sedimentation studies revealed a slow sedimentation kinetic. The decreasing of apparent surface tension is due to this slow sedimentation in the drop of the commercial particles.

The surface tension of the grafting agent alone without particles at a concentration corresponding to the initial concentration (1.3×10^{-3} mol L^{-1}) reached only 50 mN m^{-1} after 24 h and this

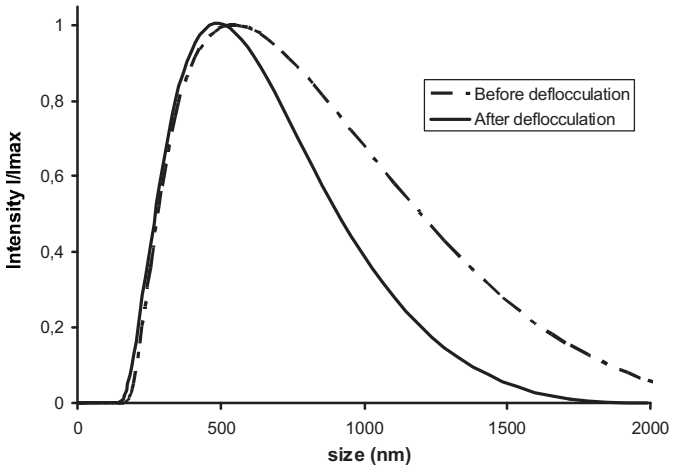

Fig. 4. Size dispersion of primary particles before and after dispersion with Ultra-Turrax (conc. 0.1 g L^{-1}).

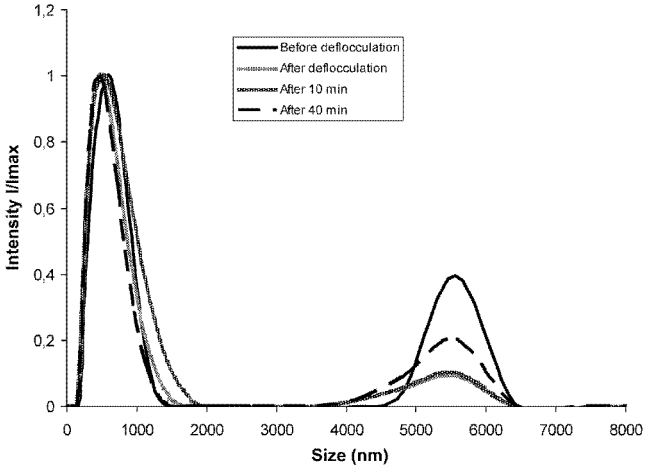

Fig. 5. Size dispersion of grafted particles before and after dispersion with Ultra-Turrax (conc. 1 g L^{-1}).

indicates that the grafting agent is a "weak" surfactant that diffuses slowly in water.

For the partially grafted particles, a relatively rapid and strong surface tension decrease is observed. In this case, complementary sedimentation studies showed that the non-aggregated particles 400 nm size sediment more slowly than the commercial ones. Just

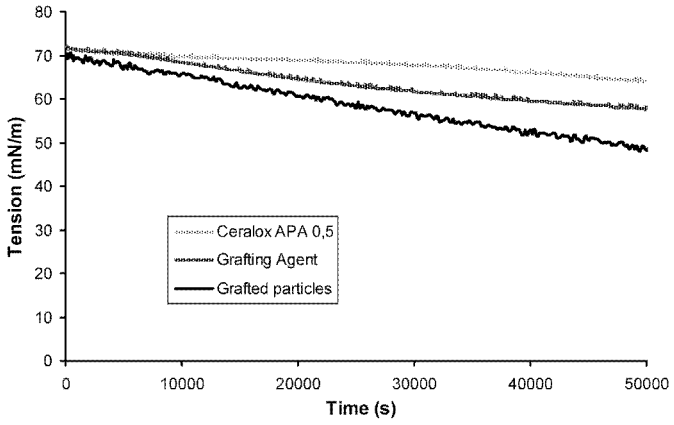

Fig. 6. Tension of grafted particles (10 g/L) compared to ungrafted particles (ceralox) and grafting agent tension at similar conditions.

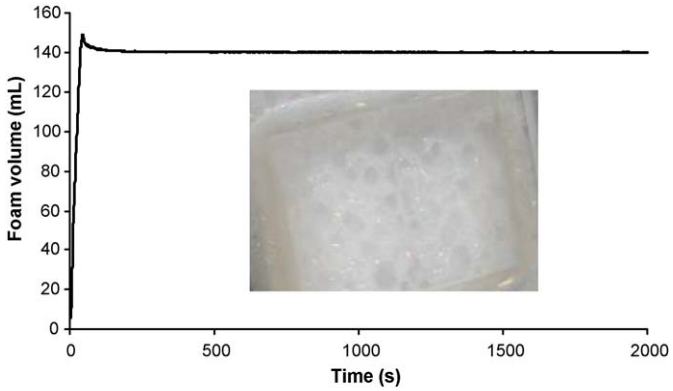

Fig. 7. Foam with an expansion ratio of 13 and volume (140 mL) obtained with 200 mL/min air flow rate.

the agglomerates (5.6 μm) could sediment more rapidly and can contribute to the strong surface tension decrease. The role of the sedimentation due to aggregation should be clarified in the future trying to suppress by pH adjustment of the suspension drop. Until now, the decrease cannot only due to the attachment of the modified particle at the air–water interface.

3.4. Foamability and drainage

The previously cited tensiometry measurements do not assume that these new fluorinated alumina particles seem to be sufficiently hydrophobic to attach to the air–water interface. It was interesting to know if foams could be generated using a concentrated dispersion of these new particles in water.

For the 0.3% weight ratio fluorinated particles, foamability tests were conducted. Compressed air at a controlled flow rate between 50–300 mL min^{-1} is diffused into 25 mL of the foaming suspension containing 100 g L^{-1} of the fluorinated particles through a removable sintered glass (porosity value of 3, 16–40 μm range) in a 2.5 cm^2 rectangular column fixed above. The generation is stopped when the foam reached a definite volume (140 mL) probed by a CCD camera (cf. Fig. 7). A couple of electrodes fixed at the bottom of the column measures the conductivity of the drained liquid remaining. A calibration performed before the experiment on the foaming suspension allows to link this conductivity to the corresponding volume and therefore to monitor the global liquid drainage out of the foam.

Extraordinary foamability was observed for three air flow rates, 50, 200 and 300 mL min^{-1}. Increasing flow rate leads to achieve initial wetter foams by ascension of water during stronger bubbling (16.76 mL for 300 mL min^{-1}) than the foam gravitational drainage (foam expansion 9.22–39.70 cf. Table 1). On a free drainage configuration, the water drained rapidly and dry foams are obtained after 3 min (cf. Fig. 8). These foams exhibit high life time more than 24 h.

Moreover, it was impossible to get foam with non-grafted Ceralox APA 0.5 particles or with only the free fluorinated short chain compound at a concentration of 1.3×10^{-3} mol L^{-1} in water whatever was the flow rate. Finally, even if the particles are washed with acetone trying to eliminate the ungrafted chains, the same foamability is reached. These new fluorinated particles grafted by

Table 1
Necessary liquid quantity to get a similar foam volume and resulting foam expansion with different gas flow rate use for the grafted particles suspension.

Gas flow rate (mL min^{-1})	200	300	50
Liquid consumed (mL min^{-1})	11.53	16.76	3.40
Foam volume (mL min^{-1})	148.86	154.54	135.09
Foam expansion	12.91	9.22	39.70

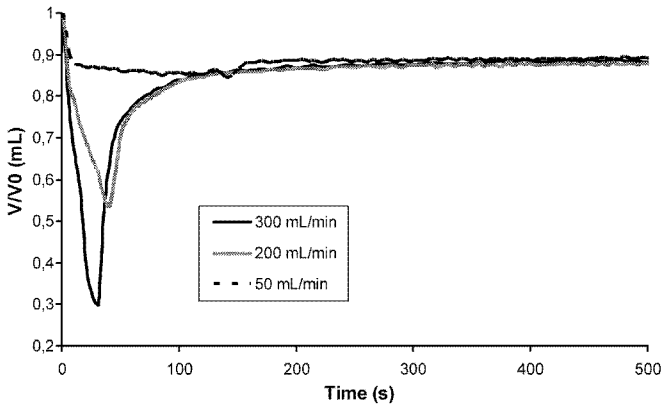

Fig. 8. Variation of the free drainage and the foam expansion with different flow rate (V: liquid volume remaining at the bottom, V_0: initial liquid volume).

covalent links are excellent candidates to attach to bubbles and stabilise foams.

4. Conclusions

This paper reports the synthesis of new foaming particles hydrophobised by partially grafting a fluorinated oligomer, CF_3–CFH–CF_2–P(O)$(OH)_2$, on commercial hydrophilic alumina particles. The short grafted chain is attached to the particles by covalent links. These particles present an excellent foamability and "Bikerman foams" could easily be generated with expansion ratio which could be greater than 20. On a free drainage configuration, relatively dry foams were obtained with a high life time more than 24 h due to the attachment of the particles at the air–water interface.

These new grafted particles will be used as models in the future to study the role of the hydrophobicity surface or grafting rate on foamability. Some investigations on the contact angle evolution as a function of the grafting rate will lead to best understand bubbles stabilisation mechanisms. The pH influence and radionuclides presence will be taken into consideration for applications in the nuclear field.

References

[1] B. Fournel, S. Faure, J. Pouvreau, C. Dame, Paper presented at the Ninth International Conference on Environmental Remediation and Radioactive Waste Management, Oxford, UK, September 21–25, 2004.
[2] S. Faure, B. Fournel, P. Fuentes, Composition, foam and method for surface decontamination, World Patent WO 2004/008463.
[3] D. Weaire, S. Hutzler, The Physics of Foam, Oxford University Press, 1999, pp. 88–101.
[4] C. Dame, C. Fritz, O. Pitois, S. Faure, Relations between physicochemical properties and instability of decontamination foams, Colloids Surf., A: Physicochem. Eng. Aspects 263 (2005) 210–218.
[5] M. Safouane, A. Saint-Jalmes, V. Bergeron, D. Langevin, Viscosity effects in foam drainage: newtonian and non-newtonian foaming fluids, Eur. Phys. J. E 19 (2006) 195–202.
[6] H.A. Wege, S. Kim, V.N. Paunov, Q. Zhong, O.D. Velev, Long-term stabilization of foams and emulsions with in-situ formed microparticles from hydrophobic cellulose, Langmuir 24 (2008) 9245–9253.
[7] S. Kim, H. Barraza, O.D. Velev, Intense and selective coloration of foams stabilized with functionalized particles, J. Mater. Chem. 19 (2009) 7043–7049.
[8] S. Fujii, P.D. Iddon, A.J. Ryan, S.P. Armes, Aqueous particulate foams stabilized solely with polymer latex particles, Langmuir 22 (2006) 7512–7520.
[9] R.J. Pugh, Foaming in chemical surfactant free aqueous dispersions of anatase (titanium dioxide) particles, Langmuir 23 (2007) 7972–7980.
[10] P.B. Binks, Particles as surfactants—similarities and differences, Curr. Opin. Colloid Interface Sci. 7 (2002) 21–41.
[11] Urs. Gonzenbach, A. Studart, E. Tervvort, L. Gauckler, Stabilization of foams with Inorganic colloîdal particles, Langmuir 23 (2006) 1025–1032.
[12] Urs. Gonzenbach, A. Studart, E. Tervvort, L. Gauckler, Tailoring the microstructure of particle-stabilized wet foams, Langmuir 23 (2007) 1025–1032.
[13] B.P. Binks, S.O. Lumsdon, Influence of particle wettability on the type and stability of surfactant-free emulsions, Langmuir 16 (2000) 8622–8631.
[14] B.P. Binks, T.S. Horozov (Eds.), Aqueous foams stabilized solely by silica nanoparticles, Angew. Chem. Int. 44 (2005) 3722–3725.
[15] R.G. Alargova, D.S. Warhadpande, V.N. Paunov, O.D. Velev, Foam superstabilization by polymer microrods, Langmuir 20 (2004) 10371–10374.
[16] Z. Nie, W. Li, M. Seo, S. Xu, E. Kumacheva, Janus and ternary particles generated by microfluidic synthesis: design, synthesis, and self-assembly, J. Am. Chem. Soc. 128 (2006) 9408–9412.
[17] S. Reculusa, C. Poncet-Legrand, A. Perro, E. Duguet, E. Bourgeat-Lami, C. Mingotaud, S. Ravaine, Hybrid dissymmetrical colloidal particles, Chem. Mater. 17 (2005) 3338–3344.
[18] A. Stocco, W. Drenckhan, E. Rio, D. Langevin, B.P. Binks, Particle-stabilised foams: an interfacial study, Soft Matter 5 (2009) 2215–2222.
[19] S. Faure, S. Guignot, New decontamination foams containing particles, French Patent n FR 07 53286, 2007.
[20] S. Guignot, S. Faure, M. Vignes-Adler, O. Pitois, Liquid and particles retention in foamed suspensions, Chem. Eng. Sci. 65 (2010) 2579–2585.
[21] P.C. Hidber, T.J. Graule, L.J. Gauckler, Influence of the dispersant structure on properties of electrostatically stabilized aqueous alumina suspensions, J. Eur. Ceram. Soc. 17 (1997) 239–249.
[22] E.S. Gawalt, M.J. Avaltroni, M.P. Danahy, B.M. Silverman, E.L. Hanson, K.S. Midwood, J.E. Schwarzbauer, J. Schwartz, Bonding Organics to ti alloys: facilitating human osteoblast attachment and spreading on surgical implant materials, Langmuir 19 (2003) 200–204.
[23] E.S. Gawalt, M.J. Avaltroni, M.P. Danahy, B.M. Silverman, E.L. Hanson, K.S. Midwood, J.E. Schwarzbauer, J. Schwartz, Bonding organics to ti alloys facilitating human osteoblast attachment and spreading on surgical implant materials corrections, Langmuir 19 (2003) 7147.
[24] R.N. Haszeldine, D.L. Hobson, D.R. Taylor, Organophosphorus chemistry. Part 19. Free-radical addition of dialkyl phosphites to polyfluoro-olefins, J. Fluor. Chem. 8 (1976) 115–121.
[25] G. Kostov, B. Ameduri, S.M. Brandstadter, Radical telomerization of 3,3,3-trifluoropropene with diethyl hydrogen phosphonate: Characterization of the first telomeric adducts and assessment of the transfer constants, J. Fluor. Chem. 128 (2007) 910–918.
[26] F. Ravera, E. Santini, G. Loglio, M. Ferrari, L. Liggieri, Effect of nanoparticles on the interfacial properties of liquid/liquid and liquid/air surface layers, J. Phys. Chem. B 110 (2006) 19543–19551.
[27] L. Liggieri, R. Miller, Relaxation of surfactants adsorption layers at liquid interfaces, Curr. Opin. Colloid Interface Sci. 15 (2010) 256–263.